JOURNAL OF BACTERIOLOGY, Nov. 1995, p. 6184–6194 Vol. 177, No. 21
0021-9193/95/$04.00+0

Genetic Evidence of a Major Role for Glucose-6-Phosphate Dehydrogenase in Nitrogen Fixation and Dark Growth of the Cyanobacterium *Nostoc* sp. Strain ATCC 29133

MICHAEL L. SUMMERS,† JAMES G. WALLIS,‡ ELSIE L. CAMPBELL, AND JOHN C. MEEKS*

Section of Microbiology, Division of Biological Sciences, University of California, Davis, California 95616

Received 26 May 1995/Accepted 17 August 1995

Heterocysts, sites of nitrogen fixation in certain filamentous cyanobacteria, are limited to a heterotrophic metabolism, rather than the photoautotrophic metabolism characteristic of cyanobacterial vegetative cells. The metabolic route of carbon catabolism in the supply of reductant to nitrogenase and for respiratory electron transport in heterocysts is unresolved. The gene (*zwf*) encoding glucose-6-phosphate dehydrogenase (G6PD), the initial enzyme of the oxidative pentose phosphate pathway, was inactivated in the heterocyst-forming, facultatively heterotrophic cyanobacterium, *Nostoc* sp. strain ATCC 29133. The *zwf* mutant strain had less than 5% of the wild-type apparent G6PD activity, while retaining wild-type rates of photoautotrophic growth with NH_4^+ and of dark O_2 uptake, but it failed to grow either under N_2-fixing conditions or in the dark with organic carbon sources. A wild-type copy of *zwf* in *trans* in the *zwf* mutant strain restored only 25% of the G6PD specific activity, but the defective N_2 fixation and dark growth phenotypes were nearly completely complemented. Transcript analysis established that *zwf* is in an operon also containing genes encoding two other enzymes of the oxidative pentose phosphate cycle, fructose-1,6-bisphosphatase and transaldolase, as well as a previously undescribed gene (designated *opcA*) that is cotranscribed with *zwf*. Inactivation of *opcA* yielded a growth phenotype identical to that of the *zwf* mutant, including a 98% decrease, relative to the wild type, in apparent G6PD specific activity. The growth phenotype and lesion in G6PD activity in the *opcA* mutant were complemented in *trans* with a wild-type copy of *opcA*. In addition, placement in *trans* of a multicopy plasmid containing the wild-type copies of both *zwf* and *opcA* in the *zwf* mutant resulted in an approximately 20-fold stimulation of G6PD activity, relative to the wild type, complete restoration of nitrogenase activity, and a slight stimulation of N_2-dependent photoautotrophic growth and fructose-supported dark growth. These results unequivocally establish that G6PD, and most likely the oxidative pentose phosphate pathway, represents the essential catabolic route for providing reductant for nitrogen fixation and respiration in differentiated heterocysts and for dark growth of vegetative cells. Moreover, the *opcA* gene product is involved by an as yet unknown mechanism in G6PD synthesis or catalytic activity.

Cyanobacteria are a morphologically diverse but phylogenetically cohesive group of gram-negative eubacteria that are phenotypically united by their oxygen-evolving photosynthetic mechanism. All cyanobacteria are photoautotrophic, using ATP and NADPH generated in the light reactions for autotrophic CO_2 assimilation by enzymes of the Calvin-Benson, or reductive pentose phosphate, cycle. They synthesize glycogen as the storage material in the light, and this glycogen is subsequently catabolized to provide maintenance energy during the dark periods of natural day-night cycles.

The vegetative cells of many filamentous cyanobacteria, such as *Nostoc* sp. strain ATCC 29133, have multiple cellular differentiation alternatives. These alternatives include heterocysts, which are the sites of N_2 fixation in the presence of O_2; spore-like akinetes, which allow survival under harsh conditions; and transiently formed, gliding, small-celled filaments called hormogonia (40). When combined nitrogen is lacking in the medium, every 10th to 20th vegetative cell along the filament may differentiate into a heterocyst. Unlike vegetative cells, terminally differentiated heterocysts lack activities of photosystem II (PSII), which is responsible for the evolution of O_2 and the generation of reducing equivalents from H_2O, and of ribulose-1,5-bisphosphate carboxylase, the primary CO_2-assimilating enzyme. Thus, heterocysts are limited to heterotrophic metabolism for the generation of reducing power and biosynthetic intermediates; ATP can be generated in the light by PSI-dependent cyclic photophosphorylation or by oxidative phosphorylation in the dark (24). The lack of PSII activity, an increase in respiratory O_2 uptake, and limited diffusion of O_2 through the unique heterocyst wall are thought to contribute to the low O_2 tension in heterocysts that is necessary for the function of O_2-sensitive nitrogenase (24). The reduction of N_2 to NH_3 by nitrogenase requires the molar equivalent of at least eight electrons and 16 ATP molecules (55). Studies describing enzyme activities and substrates capable of supporting nitrogenase activity in heterocyst extracts implicated either the initial enzymes of the oxidative pentose phosphate (OPP) pathway or those of the Embden-Meyerhof-Parnas, or glycolytic, pathway as the source(s) of reductant required for conversion of N_2 to NH_3 and for respiratory O_2 uptake (1, 5, 33, 53), with vegetative cells supplying the reduced carbon substrate (54). However, there have been neither genetic nor detailed radiotracer experiments to resolve the routes of carbon catabolism in heterocysts.

A limited number of cyanobacteria, including *Nostoc* sp. strain ATCC 29133, can grow in the dark by using glucose, fructose, or sucrose as a carbon and energy source (36, 40, 47).

* Corresponding author. Phone: (916) 752-3346. Fax: (916) 752-9014.

† Present address: Department of Plant, Soil and Environmental Sciences, Montana State University, Bozeman, MT 59717.

‡ Present address: Department of Microbiology, Molecular Biology and Biochemistry, University of Idaho, Moscow, ID 83844.

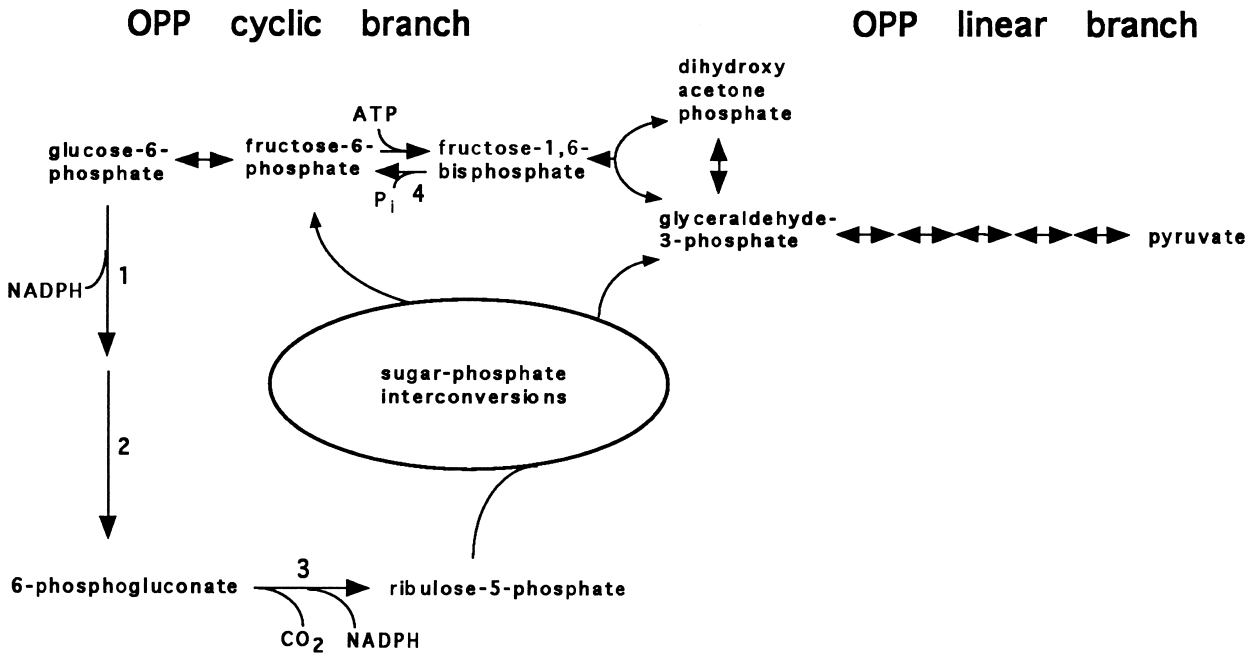

FIG. 1. A simplified scheme showing the initial three enzymes of the OPP pathway and the alternative cyclic and linear branches of the pathway. The cyclic branch illustrates regeneration of G6P, the initial substrate, while the linear branch illustrates formation of pyruvate as an end product. The numbered enzymes are as follows: 1, G6PD; 2, gluconolactonase; 3, 6PGD; and 4, fructose-1,6-bisphosphatase. The sugar-phosphate interconversions common to both oxidative and reductive pentose phosphate reactions are not individually identified, nor are the specific reactions generating NADH and ATP and leading to the formation of pyruvate from the triose phosphate intermediates. Catabolism of G6P to pyruvate via reactions of the depicted cyclic and linear branches reflects glycolysis.

Enzyme assays and radiolabeling experiments with cyanobacteria have indicated that the OPP pathway is the major, but not exclusive, route of catabolism of endogenous glycogen for dark survival or of exogenously supplied carbohydrates that provide biosynthetic intermediates for dark heterotrophic growth (28, 36–38). The NAD(P)H generated in the carbohydrate catabolism is used to synthesize ATP by oxidative phosphorylation (39).

Since activity of glucose-6-phosphate dehydrogenase (G6PD; EC 1.1.1.49) controls carbon flow into the OPP pathway in vegetative cells (see Fig. 1), we chose it to initiate a study of the pathway in *Nostoc* sp. strain ATCC 29133. G6PD catalyzes the $NADP^+$-dependent dehydrogenation of glucose-6-phosphate (G6P) to D-glucono-δ-lactone-6-phosphate (Fig. 1, enzyme 1), which is immediately hydrolyzed to 6-phosphogluconate either spontaneously or by a gluconolactonase activity (EC 3.1.1.31) (Fig. 1, enzyme 2). A second $NADP^+$-linked oxidation and decarboxylation follows, catalyzed by 6-phosphogluconate dehydrogenase (6PGD; EC 1.1.1.44) (Fig. 1, enzyme 3), which results in the production of ribulose-5-phosphate. Ribulose-5-phosphate can then enter into the sugar phosphate interconversions of the OPP pathway for synthesis of triose intermediates, which are used to regenerate G6P (Fig. 1, cyclic branch) or to synthesize pyruvate and other biosynthetic precursors (Fig. 1, linear branch).

G6PD from *Anabaena* sp. strain PCC 7120 undergoes complex regulation in which formation of more-active oligomeric forms is favored by glutamine, G6P, and low pH, as well as regulation by factors which increase catalytic activity, such as low concentrations of NADPH, ATP, and ribulose-1,5-bisphosphate (45). Furthermore, cyanobacterial G6PD may be reductively inactivated and oxidatively activated (17, 51). This thioredoxin-mediated modulation may prevent futile cycling of intermediates of the reductive and oxidative pentose phosphate pathways in the light, but it allows the OPP pathway to be active in the dark when the light-driven reduction potential drops. A 7- to 79-fold increase in G6PD activity in heterocysts relative to vegetative cells has been reported (1, 28, 53). Increased concentrations of glutamine and G6P (45), or decreased amounts of thioredoxin (16), are hypothesized to allow G6PD activity to remain high in heterocysts.

Previous genetic studies of the OPP pathway in cyanobacteria focused on the unicellular, non-nitrogen-fixing, obligate photoautotroph *Anacystis nidulans* (*Synechococcus* sp. strain PCC 6301 [40]) and yielded mutants lacking 6PGD, and both 6PGD and G6PD. The mutant phenotypes indicated that the OPP pathway was indeed the major, but not the only, pathway capable of supplying maintenance energy for darkened cells (19). The genes for G6PD (*zwf* [43]) and 6PGD (*gnd* [9]) were subsequently cloned and sequenced from *Synechococcus* sp. strain PCC 7942; *gnd* was found to be transcriptionally upregulated during the stationary phase of growth (10). Inactivation of the *zwf* gene in this strain resulted in a loss of viability upon dark incubation, but wild-type levels of dark oxygen uptake were retained (44).

We report here the results of experiments to genetically test previous biochemically derived models concerning the role of G6PD in cyanobacterial nitrogen fixation and dark heterotrophy. Mutants lacking G6PD activity were constructed by gene replacement and isolated under photoautotrophic growth conditions in the presence of NH_4^+. The phenotypic characteristics of the mutants and of strains complemented in *trans* with cloned genes provide genetic evidence that G6PD is required to support nitrogen fixation in heterocysts and dark heterotrophic growth of *Nostoc* sp. strain ATCC 29133.

MATERIALS AND METHODS

Bacterial strains, plasmids, and growth media. The plasmids and bacterial strains used in this study are listed in Table 1. *Escherichia coli* HB101 was grown

TABLE 1. Eubacterial strains and plasmids

Eubacterial strain or plasmid	Characteristics	Source or reference
Eubacterial strains		
Nostoc sp. strain ATCC 29133 (PCC 73102)	Type strain of *Nostoc punctiforme*	41
UCD 341	*Nostoc* sp. strain ATCC 29133 *zwf* Nm^r	This study
UCD 366	*Nostoc* sp. strain ATCC 29133 *opcA* Nm^r	This study
E. coli HB101	*hsdS20 recA13* (Sm) *ara14 proA2 lacY1 galK2 leuB6 xylS mtl1 supE44*	6
E. coli DH5α-MCR	*hsdR17* (r_K^- m_K^-) *recA1* Δ(*lacZYA-argF*)*U169 gyrA96 thi1 rsupE44 elA1 endA1 deoR* ϕ80d*lacZ*ΔM15 *mcrA* Δ(*mrr hsdMRS mcrBC*)	25
E. coli XL1-blue	*hsdR17 recA1 gyrA96 thi-1 supE44 relA1 lac-pro* (F′ *proAB lacI*^{q}*Z*ΔM15 Tn*10*)	Stratagene
Plasmids		
pARO191	pUC19-based cloning vector containing RP4 *oriT*; Km^r Nm^r	35
pBS KS^+	pBluescriptII KS^+, F1 *ori* pUC19-based vector for cloning and ssDNA production; Ap^r	Stratagene
pDS4101	Helper plasmid for mobilization used in triparental matings; Ap^r	50
pDUCA7	Cosmid vector with both *Nostoc* and *E. coli* origins of replication; Nm^r	12
pK184	Vector containing *nptII** lacking *Pst*I and *Sph*I sites; Nm^r	26
pRL271	Nonreplicating cyanobacterial vector containing *sacB* (13) which allows selection for gene replacement; Cm^r Em^r	Y. Cai and C. P. Wolk
pRL443	Km^s RP4 conjugal plasmid used to mobilize "cargo" plasmids; Ap^r Tc^r	20
pRL448	pRL139 containing C.K3 in *Xba*I site; source of *nptII* cassette for *zwf* gene interrupt; Ap^r Nm^r	20
pRL500	pBR320-based positive selection vector; Ap^r	20
pSCR102	pDUCA7 with ~30-kb insert of *Nostoc* genomic DNA containing *opc* operon, alias c9LF4; Nm^r	48
pSCR104	pARO191 with *nptII* replaced with *nptII** from pK184; Nm^r	This study
pSCR105	3-kb *Hin*dIII fragment of pSCR102 in *Hin*dIII site of pBS KS^+; Ap^r	This study
pSCR106	Sequencing clone containing 0.7 kb upstream of *Eag*I site within *fbp* in pBS KS^+; Ap^r	This study
pSCR110	10-kb *Sca*I fragment from pSCR102 containing entire operon in the blunted *Hin*dIII site of pRL500; Ap^r	This study
pSCR113	*zwf*::P_{psbA}*nptII* in a 10-kb fragment in pRL271; Nm^r	This study
pSCR114	*opcA*::P_{psbA}*nptII* in a 10-kb fragment in pRL271; Nm^r	This study
pSCR115	10-kb *Pst*I fragment from pSCR110 in pBS KS^+; used to make full-length ssDNA; Ap^r	This study
pSCR116	6.6-kb remaining fragment of pSCR115 after *Eco*RI digestion and ligation; used to make ssDNA for truncated S1 protection; Ap^r	This study
pSCR117	5.8-kb *Eco*RI fragment of pDCI in pBS KS^+, Ap^r	This study
pSCR119	Electroporation vector; blunted 5.8-kb *Eco*RI insert of pSCR117 in blunted *Nde*I-*Cla*I sites of pSCR104; Nm^r	This study
pSCR121	Blunted *Spe*I-*Xba*I fragment of pSCR115 containing *opcA* in *Sma*I site of pSCR202; Ap^r	This study
pSCR122	*Sph*I-*Bam*HI fragment of pSCR105 containing complete *zwf* gene in *Sph*I-*Bam*HI sites of pSCR202; Ap^r	This study
pSCR123	*Kpn*I-*Xba*I fragment of pSCR110 containing *zwf* and *opcA* in *Kpn*I-*Xba*I sites of pSCR202; Ap^r	This study
pSCR202	Electroporation vector; pSCR119 with Nm^r replaced with Ap^r	This study

in Luria broth (2), and all cloning was undertaken in either *E. coli* XL1-Blue or *E. coli* DH5α-MCR, routinely grown in 2XYT (2) or Luria-Bertani broth, respectively. Ampicillin at 100 μg/ml or kanamycin at 30 μg/ml was added to culture media when required for plasmid selection.

Nostoc sp. strain ATCC 29133 (PCC 73102; type strain of *Nostoc punctiforme* [41]) was grown in buffered liquid and agar-solidified medium as described previously (15). When needed, the medium was supplemented with neomycin at 6 or 10 μg/ml (liquid) or 10 μg/ml (solid), ampicillin at 5 μg/ml, or 5% (wt/vol) sucrose (Suc). Fixed nitrogen, when present, was supplied as 2.5 mM NH_4Cl. Growth rates were determined by increases in chlorophyll (Chl) *a* content (30) in relatively dilute cultures that were incubated at 28°C in an illuminated incubator-shaker at 250 rpm under darkness or 13 W of light per m^2 from cool-white fluorescent lamps. Medium for photoheterotrophic growth was supplemented with 10 μM 3-(3,4-dichlorophenol)-1,1-dimethylurea (DCMU) (Sigma). Prior to dark survival experiments, *Nostoc* filaments were fragmented to three to four cells per filament by using a microtip attachment of a Heat Systems Model W-225R sonicator.

***Nostoc* genomic library construction.** Total *Nostoc* sp. strain ATCC 29133 DNA was prepared as described previously (14), partially digested with *Sau*3A, size fractionated on a sucrose gradient, and ligated into the *Bam*HI site of the shuttle cosmid pDUCA7 (12). The DNA was packaged in vitro (Promega) and transfected into *E. coli* HB101. A total of 1,408 individual colonies were picked to microtiter plates for storage and replicated onto GeneScreen Plus (DuPont NEN) nylon membrane for growth, colony lysis, and blot hybridizations by standard procedures (2).

DNA methods. In vitro DNA manipulations, transformations, and restriction analyses were performed according to standard procedures (2). The Klenow fragment of DNA polymerase was used to blunt overhanging DNA ends. Ligase, Klenow fragment, S1 nuclease, and restriction enzymes were purchased from either Gibco/BRL or New England Biolabs. Single-stranded DNA (ssDNA) was synthesized from pBS KS^+-based phagemids by using R408 helper phage and purified by standard methods (Stratagene).

Plasmid and vector construction. The plasmid used to make the phagemids for production of ssDNA and for construction of insertion-inactivated genes was obtained by subcloning a 10-kb *Sca*I fragment from the cosmid clone pSCR102, containing the entire operon (48), into the blunted *Hin*dIII site of pRL500 to form pSCR110. pSCR110 was digested with *Pst*I, and the 10-kb fragment was ligated into the *Pst*I site of pBS KS^+ to form phagemid pSCR115, whose ssDNA was used in full-length S1 protection experiments. pSCR115 was digested with *Eco*RI, and the larger fragment was religated to form pSCR116 for production of ssDNA in truncated S1 protection experiments.

pSCR115 was digested with *Pml*I, which restricts only twice within the *zwf* gene, blunted, and ligated to a blunted *Xba*I P_{psbA}-*nptII* cassette from pRL448. The 10.4-kb *Sal*I-*Sst*I fragment from this plasmid containing the *nptII*-inactivated *zwf* gene was ligated into the *Xho*I-*Sst*I sites of pRL271 to form the suicide vector pSCR113. The suicide plasmid used to make the *opcA* mutant was obtained by inserting the blunted *nptII* cassette from pRL448 into pSCR115, which had been partially digested with *Bsa*HI and blunted. The resulting plasmid was confirmed by restriction analysis to contain *nptII* inserted within the *opcA* gene. The 11.1-kb *Sal*I-*Sst*I fragment containing the inactivated *opcA* gene was ligated into the *Xho*I-*Sst*I sites of pRL271 to form pSCR114.

The *Nostoc* plasmid origin of replication was isolated as a 5.8-kb *Eco*RI fragment from *Nostoc* sp. strain Mac plasmid pDC1 (27) and cloned into pBS KS^+ to form pSCR117. The portion of the shuttle vector which allows replication, antibiotic selection, and α-complementation (*lacZ*) for screening of inserts in *E. coli* was formed by ligation of *Bgl*II-*Nco*I-digested pARO191 (35) and similarly digested pK184 (26). This construct allows the use of two additional restriction enzyme sites in the multiple cloning site (MCS) by replacing the original *nptII* gene in pARO191 with *nptII** from pK184, which lacks both *Sph*I and *Pst*I sites. The resulting plasmid, pSCR104, was digested with *Nde*I-*Cla*I, the

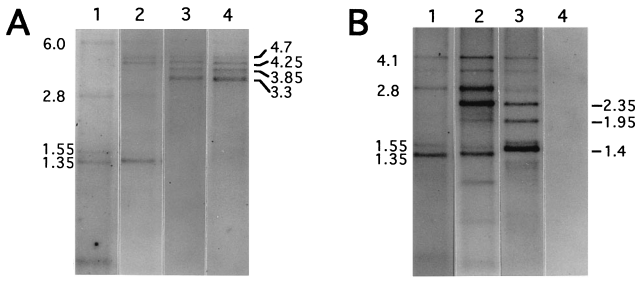

FIG. 2. Autoradiographs of full-length (A) and truncated (B) long-range nuclease protection blots of the *opc* operon. Total RNA from a nitrogen-fixing culture was protected by pSCR115 (A) or pSCR116 (B) (Fig. 4C and Table 1). Lanes 1 to 4 of panel A are autoradiographs of the same full-length S1 protection blot repeatedly hybridized with the corresponding probes for *fbp* (lane 1), *tal* (lane 2), *zwf* (lane 3), and *opcA* (lane 4). Lanes 1 to 4 of panel B are autoradiographs of the same truncated S1 protection blot probed as described for panel A.

ends were blunted, and the fragment was ligated to a similarly treated 5.8-kb *Eco*RI fragment of pSCR117 containing pDC1 to form the Km^r Nm^r shuttle vector pSCR119. An Ap^r version of this vector, pSCR202, was constructed by digestion and blunting of pSCR119 at the unique *Mlu*I site just within the pDC1 region, followed by digestion at the unique *Sal*I site within the MCS. The pDC1-containing fragment was ligated to *Ssp*I-*Sal*I-digested pUC19, and Ap^r colonies were screened for expected restriction patterns, yielding pSCR202.

Complementation vectors pSCR121, pSCR122, and pSCR123 were constructed by subcloning fragments described in Table 1 from pSCR110 into the MCS of the shuttle vector pSCR202. pSCR121 contains a 1,699-bp *Spe*I-*Xba*I fragment having 27 bp upstream of the inferred *opcA* translational start, the entire *opcA* gene, and the 274 bp downstream of *opcA* containing strong factor-independent terminators. pSCR122 contains a 2,936-bp *Sph*I-*Bam*HI fragment including 384 bp upstream of the inferred G6PD translational start, the entire *zwf* gene, and 73% of *opcA*. The 3,671-bp *Kpn*I-*Xba*I fragment in pSCR123 contains 412 bp upstream of *zwf*, both the *zwf* and *opcA* genes, and the same downstream sequence as pSCR121.

Plasmid mobilization. Triparental mating for gene replacement used pRL443 in *E. coli* HB101 to mobilize pSCR113 or pSCR114 from a pDS4101-containing *E. coli* DH5α-MCR background into *Nostoc* sp. strain ATCC 29133 as described previously (15). Plasmids based on pSCR202 were transferred into *Nostoc* sp. strain ATCC 29133 by electroporation at 8.0 kV/cm, 25 μF, and 600 Ω by using a 0.2-cm-diameter cuvette in a Bio-Rad Gene Pulser. The reaction mixture was immediately diluted with fresh medium containing NH_4^+ plus 20 mM $MgCl_2$, and electroporants were selected on solid medium after overnight recovery in liquid medium. Plasmid constructs were transformed into *E. coli* strains by standard protocols (2).

Long-range S1 protection. RNA was harvested by the method of Schmidt-Goff and Federspeil (46). RNA mapping by gel electrophoresis of endonuclease S1-resistant RNA:DNA hybrids was done as described by Favaloro et al. (23) except that 50 μg of total *Nostoc* sp. strain ATCC 29133 RNA harvested from N_2-fixing cultures was hybridized with 1 μg of ssDNA produced by pSCR115 or pSCR116 for full-length or truncated protection, respectively. Digestion with 300 U of S1 was carried out at 20°C for 90 min. Protected fragments were separated on a 1% agarose gel in Tris-borate-EDTA.

Hybridizations and probes. DNA, RNA, S1 protection, slot, and colony blots were transferred and bound to GeneScreen Plus nylon membrane, hybridized, and washed according to the manufacturer's instructions. Nucleic acids on S1 protection blots were cross-linked to the membrane by a 2.5-min exposure to UV irradiation at 7 W/m^2 by using a Fotodyne model 3-3100 transilluminator. Hybridizations were typically performed overnight in either aqueous or 50% formamide solutions at 65 or 42°C, respectively. S1 blots were stripped for reprobing by boiling for 15 min in 0.1× SSPE (1× SSPE is 0.18 M NaCl, 10 mM NaH_2PO_4, and 1 mM EDTA [pH 7.7])–2% sodium dodecyl sulfate (SDS).

DNA probes were isolated from agarose gels and radiolabeled with [^{32}P]dCTP (3,000 Ci/mmol; DuPont NEN) by using a random priming kit (Boehringer Mannheim) according to the manufacturer's directions. The probes used in this study are shown in Fig. 3A. Probe 1 was obtained as a 0.7-kb *Bss*HII fragment from sequencing clone pSCR106, probe 2 was obtained as a 0.9-kb *Hae*III fragment from pSCR110, and probes 3 and 4 were obtained as 1.4- and 1.7-kb *Spe*I fragments, respectively, from pSCR110.

Immunoblots. Cultures subjected to nitrogen step-down for subsequent SDS-polyacrylamide gel electrophoresis (PAGE) were first adapted to photoautotrophic growth in the presence of buffered NH_4Cl and 50 mM fructose, and then they were washed twice with nitrogen-free medium and placed in 50 ml of buffered medium containing 50 mM fructose. DCMU (10 μM) was added to flasks containing cultures undergoing anoxic nitrogen step-down, the flasks were sealed with serum stoppers, and the cultures were bubbled with argon for 10 min. Flasks were incubated under standard culture conditions. Cells containing a total of 10 μg of Chl *a* were harvested at 48 h after removal of combined nitrogen by 2 min of centrifugation at maximum speed in a clinical centrifuge. Cells were removed from anoxic step-down flasks with an argon-filled syringe and placed into an argon-filled centrifuge tube sealed with a serum stopper. Pellets were quickly frozen in liquid nitrogen. Proteins were extracted from cells by boiling the cell pellets for 5 min in 300 μl of 1× extraction buffer (2) and vortex mixing the samples for 5 s every minute in the presence of an equal volume of 0.5-mm-diameter glass beads. Samples were transferred to microcentrifuge tubes and centrifuged for 30 s at 16,000 × *g*. A 15-μl sample of the supernatant, corresponding to approximately 12 μg of total protein, was loaded onto an SDS–12.5% polyacrylamide gel and separated by electrophoresis using a Mini-Protean II apparatus (Bio-Rad). Proteins were transferred by electrophoresis to a nitrocellulose membrane (Hybond-ECL; Amersham) by using the Mini-Protean II Trans-Blot module and incubated with polyclonal universal antibody (diluted 1:5,000) to the Fe protein of nitrogenase; this antiserum was raised by P. W. Ludden (University of Wisconsin) against a mixture of Fe proteins from a number of nitrogen-fixing eubacteria. Visualization of the antigen-antibody conjugate was performed by luminescence (2) using horseradish peroxidase coupled to goat anti-rabbit immunoglobulin G (Cappel Organon Teknika). Protein size determinations were based on SDS-PAGE broad-range molecular markers (Bio-Rad) which were transferred to membranes, cut off prior to immunodetection, and stained with India ink (2).

Enzyme, respiration, and protein assays. G6PD activity was measured by monitoring the G6P-dependent increase in NADPH A_{340} with a Beckman Model DU70 spectrophotometer. The assay components were as described by Schaeffer and Stanier (45), except that reducing agents were omitted from both lysis and assay buffers. NADP and G6P were purchased from Sigma. Cells were concentrated to approximately 250 μg of Chl *a* per ml in a volume of 0.25 ml and disrupted in a microcentrifuge tube on ice by seven cycles of 30 s of sonication with the stepped microtip attachment described above at a setting of 1.1 and a 50% on/off cycle. Samples were incubated on ice for 1 to 2 min between periods of sonication. This treatment resulted in complete breakage of both vegetative and heterocyst cells as determined microscopically; further sonication did not change G6PD activity significantly. The crude extracts were clarified by centrifugation at 12,000 × *g* and 4°C for 5 min, and the assay was initiated by the addition of 10 μl of crude extract to the assay mixture. G6PD activity could be reductively inhibited by the addition of 2 mM dithiothreitol and oxidatively restored by the addition of 2 mM sodium tetrathionate. Protein concentration was determined by the microassay method of Bradford (7) with reagents from Bio-Rad.

Dark O_2 uptake was measured at 25°C by using a Clark-type oxygen electrode with a 2-ml chamber. No attempt to measure O_2 uptake in the light was made. Cells were harvested from exponential-phase cultures and assayed immediately at a concentration of 20 to 40 μg of Chl *a* per ml. Whole-cell acetylene reduction to ethylene as a measure of nitrogenase activity was assayed by gas chromatography (30). Student's *t* distribution was used to determine the statistical significance of rate determinations.

RESULTS

Identification of the *opc* operon. The cloning, nucleotide sequence, and organization of the 6,672-bp *Dra*I-*Xba*I region of *Nostoc* sp. strain ATCC 29133 genomic DNA have been reported previously (48) (Genome Sequence Database accession no. L32796). This region contains four open reading

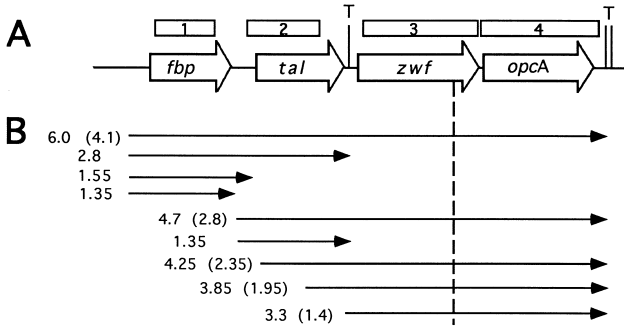

FIG. 3. Hybridization probes (A) and approximate locations of transcript endpoints (B) of the *opc* operon. Transcript sizes are shown in kilobases, and sizes of truncated protection fragments are in parentheses. Probes 1 to 4 are described in the text. T denotes factor-independent terminators identified by sequence analysis. The vertical dashed line shows the 3′ limit of truncated transcript protection by pSCR116.

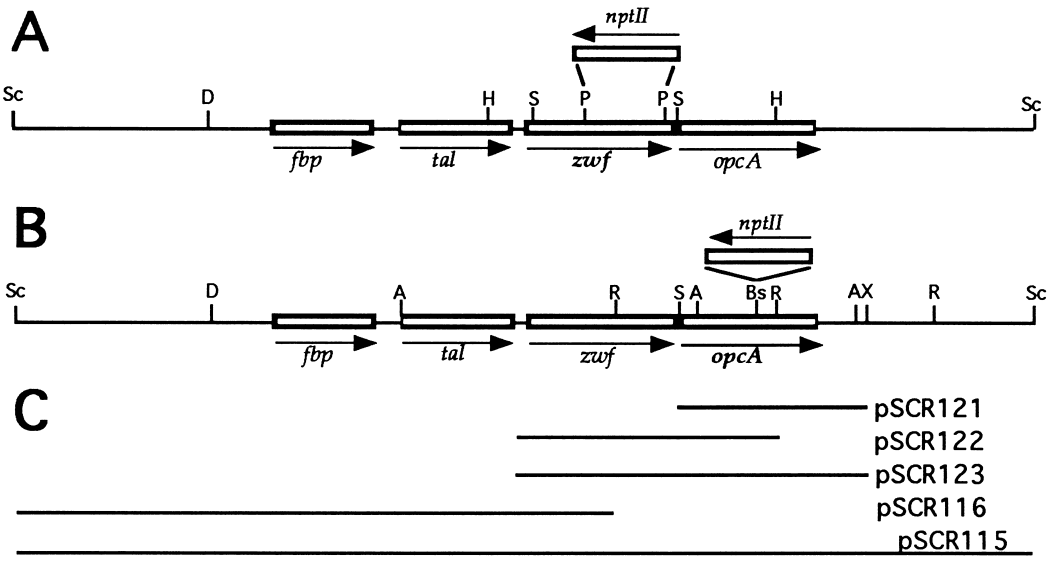

FIG. 4. Gene inactivations used to construct strains UCD 341 and UCD 366 and fragments used for complementation and S1 nuclease analysis. The structures of the *opc* operon regions of strain UCD 341, showing the deletion of a 679-bp *Pml*I fragment and its replacement by an *nptII* cassette (A), and strain UCD 366, showing the insertion of an *nptII* cassette in the *Bsa*HI site within *opcA* (B), are presented. (C) Fragments used for genetic complementation and ssDNA generation, described in Table 1 and the text. Arrows indicate the direction of transcription. Abbreviations for restriction endonucleases: A, *Acc*I; Bs, *Bsa*HI; D, *Dra*I; H, *Hin*dIII; P, *Pml*I; R, *Eco*RV; S, *Spe*I; Sc, *Sca*I; X, *Xba*I.

frames encoding fructose-1,6-bisphosphatase (*fbp*), transaldolase (*tal*), and G6PD (*zwf*), which were provisionally identified by analysis of sequence similarity, plus an unidentified open reading frame given the provisional name *opcA* to indicate its involvement in the OPP cycle. Long-range S1 nuclease protection blots were used to establish transcriptional linkage in this region (see below). While it is not inclusive of all genes of the cyclic pathway, we have designated this operon *opc.*

Full-length transcript protection offered by ssDNA generated from pSCR115 that is complementary to the mRNA produced by this region, and which allows approximate determination of size and the 5′ and 3′ ends of transcripts, is shown in Fig. 2A. The four lanes show autoradiographs of the same blot sequentially probed with genes in the proposed operon; the previous hybridizing probe was removed completely prior to subsequent probing. Blot hybridization with the *zwf* probe (Fig. 3A, probe 3) revealed a series of transcripts of 3.3, 3.85, 4.25, 4.7, and 6.0 kb. Hybridization with *opcA* (probe 4) revealed an identical series of transcripts with the addition of a very faint 1.5-kb band. Probe 2, encoding *tal*, identified the 4.25-, 4.7-, and 6.0-kb transcripts, as well as smaller 1.35- and 2.8-kb transcripts most likely encoding *tal* and *fbp-tal*, respectively. The 3.85-kb transcript was only faintly seen, probably because of the small overlap (<100 bp) between the probe and the predicted position of this transcript. The *fbp* probe (probe 1) identified the 6.0-kb transcript, as well as 1.35- and 1.55-kb transcripts most likely encoding *fbp* alone and the 2.8-kb transcript for *fbp-tal* previously identified with probe 2. On the basis of the probe specificity and sizes of the larger transcripts, we propose cotranscription of *fbp-tal-zwf-opcA* for the 6.0-kb transcript, of *tal-zwf-opcA* for the 4.7-kb transcript, and of *zwf-opcA* for the 4.25-, 3.85-, and 3.3-kb transcripts. If it is assumed that all of the larger transcripts terminate at a single site, a model depicting multiple 5′ ends can be made (Fig. 3B).

Support for this model comes from an S1 protection experiment which used a truncated ssDNA fragment from pSCR116 for mRNA protection. This complementary ssDNA hybridizes with the 5′ portion of the larger transcripts from the *Eco*RI site within *zwf*; thus, the protected fragment corresponds to the distance from the *Eco*RI site to the 5′ end of the transcript. The blot of these separated protection fragments was probed as described above (Fig. 2B). Apart from the smaller, upstream transcripts also present in the full-length blot, each of the truncated larger transcripts corresponds to a full-length transcript, if it is assumed that the larger transcripts terminate at approximately 1.9 kb downstream of the *Eco*RI site in *zwf* (compare Fig. 2A and 2B). Thus, the 6.0-, 4.7-, and 3.3-kb transcript bands in Fig. 2A correspond to 4.1-, 2.8-, and 1.4-kb bands, respectively, in Fig. 2B. These examples, and other proposed transcript locations, are illustrated in Fig. 3B, in which the size of the truncated protection fragment observed in Fig. 2B is given in parentheses beside that of the full-length transcript as seen in Fig. 2A.

Additional evidence for this model comes from sequence analysis. By using the Terminator algorithm of Brendel and Trifonov (8), strong factor-independent transcriptional terminators were identified; a pair occur just downstream of *opcA* at positions 6494 and 6581, which correspond approximately to the 3′ ends of the larger transcripts. A third terminator, which most likely terminates the 1.35-kb *tal* and 2.8-kb *fbp-tal* transcripts, was detected between *tal* and *zwf* at position 3346 (T in Fig. 3A). Similar terminator sequences to account for the proposed 1.35- and 1.55-kb *fbp* transcripts were not obvious in the region between *fbp* and *tal.*

Gene inactivations. To analyze the role of G6PD in *Nostoc* sp. strain ATCC 29133, a *zwf* mutant was constructed. The wild-type genomic region showing the replacement of a 0.7-kb *Pml*I fragment within *zwf* with a 1.1-kb *nptII* cassette from pRL448 is shown in Fig. 4A. Putative double recombinant *Nostoc* sp. strain ATCC 29133 clones were selected for both Nm^r and Suc^r under photoautotrophic growth conditions with NH_4^+ as the nitrogen source. The DNA of a representative clone, UCD 341, was extracted and analyzed by Southern hybridization using a *zwf* probe (Fig. 3A, probe 3). The results presented in Fig. 5A show that *Spe*I and *Hin*dIII fragments containing the *zwf* gene in strain UCD 341 had increased by 0.4

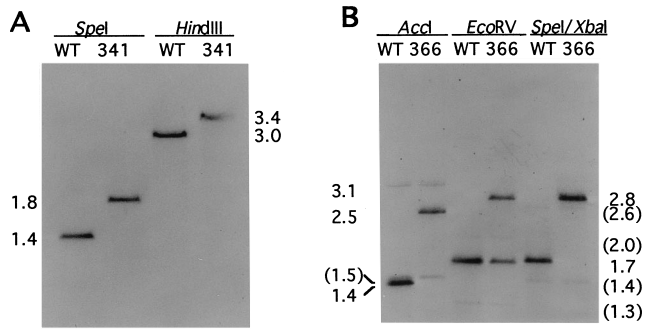

FIG. 5. Confirmation of gene replacement in strains UCD 341 and UCD 366. (A) Wild-type (WT) and UCD 341 strains digested with *Spe*I or *Hin*dIII and probed with the *zwf* gene (Fig. 3A, probe 3). (B) Wild-type and UCD 366 strains digested with *Acc*I, *Eco*RV, or *Spe*I-*Xba*I and probed with the *opcA* gene (Fig. 3A, probe 4). Sizes are in kilobases.

kb in comparison with the wild type, as predicted by the deletion-insertion. No other hybridizing bands were observed in either mutant or wild-type lanes, verifying gene replacement by homologous recombination in strain UCD 341 and indicating that *zwf* is present as a single copy in the genome of *Nostoc* sp. strain ATCC 21933.

A gene inactivation was also constructed by insertion of the *nptII* cassette into the *Bsa*HI site within *opcA* (Fig. 4B), and double recombinants were selected as described for strain UCD 341. A putative double recombinant *opcA* mutant, strain UCD 366, was analyzed by Southern hybridization using the *opcA* probe (Fig. 3A, probe 4). Restriction fragments hybridizing strongly with *opcA* from strain UCD 366, generated with *Acc*I, *Eco*RV, and *Spe*I-*Xba*I, all increased by 1.1 kb compared with the wild type (Fig. 5B), as predicted by the insertion and gene replacement. Probe 4 overlaps a portion of a 3.1-kb *Acc*I fragment extending upstream and a portion of a 1.7-kb *Eco*RV fragment extending downstream of *opcA*. The presence of additional hybridizing fragments of identical size in the wild-type and mutant lanes for each digest implies that at least one other copy of this or a homologous gene is present in the *Nostoc* sp. strain ATCC 29133 genome (Fig. 5B; sizes shown in parentheses).

Phenotypic analysis of *zwf* mutant strain UCD 341. G6PD activity in crude extracts of the wild-type strain was twofold higher for N_2-grown cells than for NH_4^+-grown cells (Table 2). The apparent G6PD activity in the *zwf* mutant strain UCD 341 was 5 to 7% of that of the wild type when the strains were grown photoautotrophically under permissive conditions with NH_4^+ or after a shift to incubation with N_2 in the absence of NH_4^+ (Table 2). Treatment of cell extracts with sodium tetrathionate did not increase the activity, indicating that the low rates were not a consequence of reductive inactivation of G6PD. Strain UCD 341 was unable to grow in the absence of combined nitrogen. Acetylene is an alternative substrate for nitrogenase; as determined by whole-cell assay, nitrogenase activity was absent in the *zwf* mutant (Table 2). Light microscopy showed no evidence of abnormal heterocyst morphology, frequency, or spacing in the mutant filaments (photomicrographs not shown).

We propose that the loss of nitrogenase activity was due to a lack of reductant normally supplied by the OPP cycle. Addition of the strong reducing agent sodium dithionite to samples taken from a culture at 48 h after a nitrogen step-down in air and assayed in the absence of O_2 resulted in about 10% of the wild-type acetylene-reducing activity for strain UCD 341. To circumvent any O_2 inactivation of newly synthesized nitrogenase, possibly caused by the lack of respiratory O_2 uptake in the heterocysts of strain UCD 341, cultures were similarly

TABLE 2. Phenotypic characteristics of wild-type *Nostoc* sp. strain ATCC 29133, mutant strain UCD 341, and genetic complemented strains of UCD 341

Parameter	Growth conditions[a]	Value for strain[b]:			
		ATCC 29133	UCD 341	UCD 341/pSCR122	UCD 341/pSCR123
Doubling time (h)					
Photoautotrophy	Light, N_2	26 ± 1.6	NG[c]	27 ± 1.5	22 ± 1.0
	Light, NH_4^+	16 ± 0.6	17 ± 1.4	19 ± 1.1	19 ± 1.0
Photoheterotrophy	Light, DCMU, fructose, CAA, NH_4^+	39 ± 2.0	45 ± 1.8	38 ± 1.5	37 ± 0.7
Dark heterotrophy	Dark, fructose, CAA, NH_4^+	39 ± 2.7	NG	47 ± 2.8	33 ± 1.5
G6PD activity, photoautotrophy[d]	Light, N_2	63 ± 7.5	4.7 ± 0.27[e]	16 ± 0.17	1160 ± 56
	Light, NH_4^+	31 ± 0.04	1.6 ± 0.40	8.0 ± 0.07	709 ± 59
Dark respiration[f]					
Photoautotrophy	Light, NH_4^+	1.1 ± 0.25	1.6 ± 0.41	1.8 ± 0.36	3.4 ± 0.38
Phototrophy	Light, fructose, CAA, NH_4^+	3.3 ± 0.34	1.9 ± 0.10	2.4 ± 0.40	3.5 ± 0.25
Acetylene reduction, photoautotrophy[g]	Light, N_2	372 ± 7.0	0	308 ± 10	398 ± 26

[a] Buffered liquid minimal medium had either no (N_2) or 2.5 mM NH_4^+ added as indicated and 50 mM fructose plus 0.5 g of CAA per liter for heterotrophic growth. Photoheterotrophic growth is defined as growth in the presence of 10 μM DCMU. The fractional utilization of CO_2 and fructose as biosynthetic carbon sources in the presence of light and the absence of DCMU was not determined, and thus this phototrophic growth mode is not qualified (autotrophic or heterotrophic) with respect to the carbon source. In the absence of CAA, the doubling times of the wild type were approximately 96 and 55 h under photoheterotrophic and dark heterotrophic conditions, respectively.

[b] Values for G6PD activity are means ± standard deviations (SD) for two separate experiments. Values for all other parameters are means ± standard errors (SE) for three or more separate experiments.

[c] NG, no growth.

[d] Nanomoles of NADPH produced per min per mg of protein.

[e] N_2-incubated rates for strain UCD 341 reported as means ± SE for three time points following nitrogen step-down were as follows: 22 h, 4.67 ± 0.23; 46 h, 5.2 ± 0.18; and 70 h, 4.21 ± 0.66 (each as the mean ± SD for two replicates).

[f] Nanomoles of O_2 uptake per min per mg of protein.

[g] Nanomoles of ethylene formed per min per mg of Chl *a*.

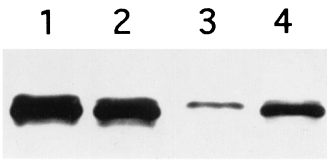

FIG. 6. Immunoblot of dinitrogenase reductase (Fe protein) in extracts from *Nostoc* sp. strain ATCC 29133 (lanes 1 and 2) and *zwf* mutant strain UCD 341 (lanes 3 and 4) separated by SDS-PAGE. Extracts in lanes 1 and 3 were obtained from cells at 48 h after nitrogen step-down in air (oxic). Extracts in lanes 2 and 4 were obtained from cells at 48 h after nitrogen step-down in the absence of air and the presence of argon (anoxic). The autoradiogram detecting the chemiluminescent signal was exposed for 1 min.

assayed after anoxic nitrogen step-down in the presence of argon, 50 mM fructose, and 10 μM DCMU to block photosynthetic O_2 production; no stimulation of acetylene-reducing activity occurred relative to nitrogen step-down in air.

To determine whether the amounts and structures of nitrogenase subunits were comparable in mutant and wild-type strains, proteins in cell extracts were separated by SDS-PAGE and immunoblots were probed with a universal dinitrogenase reductase (Fe protein) antiserum (Fig. 6). A cross-reactive band was present in extracts of the wild-type strain and the *zwf* mutant UCD 341 following both oxic and anoxic nitrogen step-down, establishing the presence of dinitrogenase reductase. Densitometer analysis of the blots shown in Fig. 6 indicated that approximately fivefold more dinitrogenase reductase protein was present in the mutant strain under anoxic conditions relative to oxic conditions and that under oxic and anoxic incubation conditions approximately 1/10 and 1/2, respectively, of the dinitrogenase reductase was present in the mutant relative to the wild-type strain. Two forms of dinitrogenase reductase have been observed in cyanobacteria, with the presence of a more slowly migrating, higher-molecular-mass form usually emerging under conditions which inactivate nitrogenase, such as high O_2 or NH_4^+ concentrations (22, 56). Although slight differences in migration could be seen in the oxic and anoxic extracts of both mutant and wild-type cultures, two or more cross-reactive bands were not resolved (Fig. 6).

The *zwf* mutant also failed to grow in the dark on fructose or any other carbon source (Table 2). Metabolic intermediates such as the five-carbon sugars used in nucleic acid synthesis, which are normally produced by the OPP cycle in the dark, might be expected to be limiting in a G6PD mutant. However, neither ribose nor xylose in the presence of fructose alleviated the dark growth defect (Table 3). Addition of Casamino Acids (CAA) to the fructose-based medium was expected to decrease demands for amino acid biosynthesis. The growth rate of the wild-type strain increased significantly in the presence of CAA, but CAA were unable to support dark growth of the mutant strain. Combinations of five-carbon sugars and CAA were also without effect.

Dark survival in cultures placed in buffered medium containing NH_4^+, with and without 50 mM fructose, was monitored. In the absence of an exogenous carbon source, only 0.2% of the wild-type cells and none of the mutant cells survived after 7 days of dark incubation. Addition of fructose resulted in nearly constant viability for both mutant and wild-type strains over 3 weeks of dark incubation, as determined by the CFU on plates incubated under photoautotrophic growth conditions. Microscopy revealed that the number of cells per filament increased for the wild-type strain in a manner corresponding to the doubling time observed under these conditions, but because the filaments did not fragment and a filament is equivalent to a CFU, this growth was not reflected when growth was assayed by colony counts. Such an increase in cells per filament was not observed for strain UCD 341; in fact, over 50% of the cells in these filaments had differentiated into akinetes. Germination of the akinetes under permissive growth conditions (photoautotrophic growth with NH_4^+) on plates accounts for the dark viability of mutant strain UCD 341.

Fructose-supported photoheterotrophic growth was obtained by the addition of DCMU to the growth medium. DCMU blocks production of NADPH by noncyclic electron flow from PSII through PSI, but it does not prevent ATP from being generated by PSI-mediated cyclic photophosphorylation (11). The photoheterotrophic doubling time for strain UCD 341 of 45 ± 1.8 h (Table 2) showed a small but significant difference ($P > 0.8$) from the doubling time of 39 ± 2.0 h for the wild type, presumably because reactions other than the OPP pathway were less efficient in supplying biosynthetic intermediates from fructose in the mutant strain.

The rate of dark O_2 uptake was slightly higher in strain UCD 341 than in the wild type when photoautotrophic, NH_4^+-grown cells were assayed immediately after transfer to the dark (Table 2). No estimates of O_2 uptake in the light were made, because photosynthetic O_2 evolution exceeds any uptake by at least an order of magnitude. After cells were grown for 4 days phototrophically in the presence of fructose, the rate of dark O_2 uptake in the wild-type culture increased approximately threefold, while the *zwf* mutant strain UCD 341 showed no significant increase.

Genetic complementation of *zwf* mutant strain UCD 341. To subclone complementing fragments into an Nm^r *Nostoc* strain, the vector pSCR202 was constructed by combining *Nostoc* and *E. coli* replicons (see details in Materials and Methods). This pUC19-based Ap^r electroporation vector has 11 restriction enzyme sites in the MCS and allows α-complementation (β-galactosidase) screening for inserts in *E. coli*. On the basis of densitometric measurement of autoradiographs resulting from slot blot hybridizations with normalized total DNA, the copy number of plasmids containing the replicon within the 5.8-kb pDC1 fragment is approximately 14 per chromosome in *Nostoc* sp. strain ATCC 29133. This value was found to remain constant for inserts up to 10 kb in length (data not shown).

The *zwf* mutant strain UCD 341 was complemented by plas-

TABLE 3. Photoheterotrophic and dark heterotrophic growth of wild-type *Nostoc* sp. strain ATCC 29133 and *zwf* mutant strain UCD 341 in the presence of ammonium, fructose, and various supplements

Growth conditions and supplement(s)	Strain doubling time (h)[a]	
	ATCC 29133	UCD 341
Photoheterotrophy		
CAA	39 ± 2.0	45 ± 2.0
CAA plus 10 mM ribose	42 ± 0.4	44 ± 1.0
CAA plus 10 mM (each) ribose and xylose	36 ± 0.7	39 ± 0.5
Dark heterotrophy		
10 mM ribose	60 ± 0.7	NG[b]
10 mM (each) ribose and xylose	55 ± 0.05	NG
CAA	39 ± 3.0	NG
CAA plus 10 mM ribose	31 ± 0.8	NG
CAA plus 10 mM (each) ribose and xylose	44 ± 1.3	NG

[a] Doubling time in liquid culture. Values are the mean ± standard errors for at least three separate experiments. Buffered medium was supplemented with 2.5 mM NH_4Cl, 50 mM fructose, 0.5 g of CAA per liter, and/or five-carbon sugars as indicated, and for photoheterotrophic growth, 10 μM DCMU was added.

[b] NG, no growth.

mids pSCR122 (*zwf*) and pSCR123 (*zwf opcA*) but not by pSCR121 (*opcA*) (Fig. 4C). The presence of pSCR122 (*zwf*) in strain UCD 341 restored approximately 25% of the wild-type in vitro G6PD activity, with the restored activity being higher in N_2-grown cultures than in NH_4^+-grown cultures (Table 2); sodium tetrathionate oxidation of cell extracts did not increase activity. This partial complementation of catalytic activity allowed complete restoration of the wild-type photoautotrophic growth rate under nitrogen-fixing conditions, accompanied by restoration of near wild-type levels (83%) of acetylene-reducing activity. The slight defect in photoheterotrophic growth observed for strain UCD 341 was also corrected by the presence of pSCR122 (*zwf*). The dark heterotrophic growth defect was restored by pSCR122 (*zwf*) to 83% of the wild-type rate. In a manner similar to that for strain UCD 341 alone, levels of dark respiratory O_2 uptake were slightly higher than wild-type levels in NH_4^+-grown cells and showed only a slight increase when fructose was added to the medium.

Complementation with both *zwf* and *opcA* in multicopy pSCR 123 increased G6PD catalytic activity 23- and 18-fold over rates for the wild type grown with NH_4^+ and N_2, respectively (Table 2). The increased G6PD activity did not affect photoautotrophic growth in NH_4^+, but growth with N_2 as the sole source of nitrogen was 1.2-fold faster than that of the wild type. The increased growth rate was paralleled by a small increase in the rate of acetylene reduction. The slight defect in photoheterotrophic growth observed for strain UCD 341 was also corrected by the presence of pSCR123 (*zwf opcA*), although there was no stimulation of the growth rate beyond that of the wild-type strain. The rate of dark heterotrophic growth of strain UCD 341 bearing pSCR123 (*zwf opcA*) increased 1.2-fold over the wild-type rate to a generation time of approximately 33 h. The rate of dark respiration for the pSCR123 (*zwf opcA*)-complemented mutant was approximately threefold higher in photoautotrophic, NH_4^+-grown cultures relative to the wild type and was similar to the rates observed for both this strain and the wild type when grown in the presence of fructose.

The lack of complementation in *trans* of the *zwf* mutant by pSCR121 (*opcA*) indicates that the defective N_2-dependent and dark growth phenotype was not a singular consequence of polar inactivation of *opcA*.

Phenotypic analysis and genetic complementation of *opcA* mutant strain UCD 366. The phenotype of *opcA* mutant strain UCD 366 was similar to that of *zwf* mutant strain UCD 341. Strain UCD 366 grew in a manner identical to that of the wild type under photoautotrophic conditions with NH_4^+, but it failed to grow with N_2 as the sole nitrogen source or in the dark with fructose. Apparent G6PD activity was 2% of that of the wild type in NH_4^+-grown cultures.

The growth phenotypes of strain UCD 366 were complemented in *trans* by pSCR121 (*opcA*) but not by pSCR122 (*zwf*) or pSCR202, the vector control. The presence of pSCR121 (*opcA*) in NH_4^+-grown cells restored G6PD activity (34.7 ± 9.8 nmol of NADPH produced per min per mg of protein) to wild-type levels (Table 2). There was no indication of an *opcA*-specific transcript in RNA or S1 blots. Transcription of *opcA* in pSCR121 could have been initiated from the *lacZ* promoter in the vector or from a weak native promoter not visible in wild-type RNA that allowed complementation when present on a multicopy plasmid.

DISCUSSION

On the basis of mRNA analysis, the G6PD structural gene in *Nostoc* sp. strain ATCC 29133 is part of a four-gene operon encoding proteins of the OPP cycle in the order *fbp-tal-zwf-opcA*. Cotranscription of these four genes in an operon (Fig. 3B) is consistent with the corresponding enzymes operating in a cyclic pathway. Fructose-1,6-biphosphatase dephosphorylation activity (Fig. 1, enzyme 4) would shift metabolism of the triose phosphate intermediates (glyceraldehyde-3-phosphate in equilibrium with dihydroxyacetone phosphate) in the direction of G6P formation (Fig. 1, cyclic branch) as opposed to formation of pyruvate in a linear pathway (Fig. 1, linear branch). Large amounts of NADPH could then be produced from a small amount of supplied carbohydrate, as would be required for nitrogen fixation in the heterocyst and for ATP generation by oxidative phosphorylation in the dark. Cotranscription also of three genes (*tal-zwf-opcA*) and gene pairs (*fbp-tal* and *zwf-opcA*) or of single genes (*fbp* or *tal*) (Fig. 3B) implies flexibility in the synthesis of catabolic enzymes in response to specific metabolic demands in *Nostoc* sp. strain ATCC 29133. The increase in G6PD activity in N_2-grown cells relative to NH_4^+-grown cells of the wild type and complemented mutants also implies flexibility in response to growth conditions. Cyanobacteria have long been assumed not to have such carbon metabolic adaptability (18).

The role of G6PD in heterocyst metabolism. Results of enzymatic studies of vegetative cell and heterocyst fractions have not resolved the question of whether glycolysis or the OPP cycle, or both, supplies reductant in heterocysts (4, 24). On the basis of the characteristics of *zwf* mutant strain UCD 341 and *opcA* mutant strain UCD 366, we suggest that G6PD and the OPP cycle are essential for electron donation in heterocysts for both respiratory O_2 uptake and N_2 reduction.

Loss of reductant supply for either respiratory electron transport or nitrogenase should result in a defect in N_2 fixation. Respiratory O_2 uptake in heterocysts contributes both to the creation of an anoxic environment allowing the O_2-labile nitrogenase to function (21) and to ATP generation in the dark. If catalytically active nitrogenase in strain UCD 341 was limited only by reductant supply, the activity should have been enhanced by the exogenous artificial reductant dithionite. However, dithionite restored only a fraction of the wild-type nitrogenase activity following nitrogen step-down under either oxic or anoxic conditions when this activity was assayed in an anoxic environment. There are three possible explanations for these results. First, there was limited synthesis of nitrogenase in the mutant strain; second, nitrogenase was synthesized but existed in a predominantly inactive form; or third, dithionite was unable to enter the attached heterocysts. Immunoblots were used to test the first two possibilities. Dinitrogenase reductase was synthesized in *zwf* mutant strain UCD 341, but it accumulated at levels significantly lower than those at which it accumulated in the wild-type strain even under anoxic conditions, which protect against O_2 inhibition of transcription. This result may reflect an indirect effect of limited reductant supply influencing transcription, mRNA stability, or stability of this protein. The greater accumulation of dinitrogenase reductase under anoxic conditions relative to oxic conditions in the mutant is consistent with the idea that G6PD provides reductant to sustain O_2 uptake in heterocysts, which in turn contributes to the low O_2 tension in these cells and decreases O_2 inhibition of synthesis. The inability to clearly resolve multiple forms of dinitrogenase reductase does not support the presence of active and inactive forms of the enzyme in the mutant. The observation that, following oxic nitrogen step-down, dithionite supported acetylene reduction in strain UCD 341 at a rate proportional to that of the amount of dinitrogenase reductase present implies that dithionite entered the attached heterocysts. We cannot, however, explain why dithionite did not support proportionally higher acetylene reducing activity follow-

ing anoxic nitrogen step-down in cultures that appeared to contain fivefold-more dinitrogenase protein. We can only speculate that factors other than the amount and state of dinitrogenase reductase contribute to the N_2 fixation defect in the *zwf* mutant. Nevertheless, the loss of nitrogenase activity in the *zwf* mutant is consistent with a decreased supply of reductant in heterocysts that cannot be supplemented by other metabolic reactions, such as carbon flux from the glycolytic pathway to pyruvate (Fig. 1) and then to α-ketoglutarate, which would yield reduced ferredoxin and NADPH (5, 34).

We found no molecular genetic evidence for a second *zwf* gene in addition to that in the *opc* operon and have no facile explanation for the low level of G6P-dependent NADPH production in extracts of *zwf* mutant strain UCD 341. The residual G6PD activity in strains UCD 341 and UCD 366 could reflect the presence of an alternative G6PD, encoded by a heterocyst-specific gene with low-level sequence similarity to *zwf*, as has been suggested for *Anabaena* sp. strain PCC 7120 (3). However, if present in *Nostoc* sp. strain ATCC 29133, this activity was not sufficient to support N_2 fixation.

Complementation of strain UCD 341 with pSCR122 (*zwf*) restored only 25% of the wild-type G6PD activity, but it allowed almost complete complementation of the mutant acetylene reduction activity (83%) and N_2 growth defect (96%). This amount of enzyme activity is thus sufficient to supply the reductant needs within the heterocyst for near-maximal nitrogenase activity. Therefore, one can conclude that the activity of G6PD is not likely to be severely limiting for N_2 fixation in wild-type cells. When an intact *opcA* gene was also present on the complementing fragment as in pSCR123, in vitro catalytic activities of G6PD increased in a somewhat higher proportion than expected if caused by a gene dose effect due to the multicopy plasmid to between 18 and 23 times the wild-type rates. The increased G6PD activity allowed a small (18%) increase in growth rate on N_2, perhaps arising from a slight (7%) increase in nitrogenase activity. The results of these complementation experiments provide strong evidence for the essential role of G6PD and the OPP cycle in carbon catabolism and reductant supply to nitrogenase in these highly differentiated cells.

The role of G6PD in heterotrophic growth. G6PD is also required for dark heterotrophic growth of vegetative cells. The *zwf* (and *opcA*) mutant strain could not grow in the dark on fructose (or glucose; data not shown), even when supplemented with CAA or five-carbon sugars which, if acting as precursors, could supply missing metabolic intermediates required for growth. It is possible that failure to transport these substrates into the cell or to phosphorylate them once in the cell contributed to the lack of dark growth. We suggest that transport limitation is unlikely because an increase in dark growth was observed for the wild type in the presence of these additions and for the mutant strain during photoheterotrophic growth (Table 3). These results indicate that the lack of dark growth by the *zwf* mutant was not entirely due to the absence of activated metabolic intermediates and that some other factor(s) may be limiting.

Since little reductant is required for biosynthesis during dark heterotrophy, cellular ATP might be a factor limiting growth of cyanobacteria under these conditions (47). Evidence that the OPP cycle functions in the supply of reductant for oxidative phosphorylation in vegetative cells is provided here by, relative to the wild type, the correlations between increased and decreased G6PD activity, dark growth rate, and respiration rate for the pSCR123 (*zwf opcA*)- and pSCR122 (*zwf*)-complemented *zwf* mutants, respectively (Table 2). The threefold stimulation of the respiration rate in both the wild-type strain in the presence of fructose and the pSCR123-complemented strain UCD 341 may reflect the capacity to generate the additional ATP required for heterotrophic growth. ATP limitation is supported by the observation that while the *zwf* mutant could not grow in the dark, its growth rate in photoheterotrophic culture, i.e., under conditions in which ATP levels are high because of cyclic photophosphorylation, was 87% of that of the wild type. Induction of akinetes in *Nostoc* sp. strain PCC 7524 has been linked to a cellular decline in energy charge (49). The induction of akinete formation in strain UCD 341 under dark heterotrophy implies that ATP was limiting under these conditions. We interpret these collective results as indicating that under dark heterotrophic growth conditions, the *zwf* mutant could not generate enough reductant to supply ATP at levels sufficient to allow growth or to suppress the induction of akinete differentiation.

The observation that NH_4^+-grown strain UCD 341 had a rate of dark respiration that was similar to the wild-type rate indicates that the OPP cycle is not the only pathway for reductant generation in this strain. Since measurements of O_2 uptake were done with photoautotrophic cultures immediately transferred to dark incubation conditions, it is possible that photosynthate pools could provide reductant for respiration over a short term. However, all the enzymes for a complete glycolytic pathway have been detected in three cyanobacteria (31, 32, 42). The glycolytic pathway has also been implicated in anaerobic fermentation by cyanobacteria (29, 31, 52), and it is thus the most probable pathway supplying reductant for the observed dark respiration in the *zwf* mutant strain UCD 341.

The role of *opcA*. There are two major lines of evidence that indicate that *opcA* is required for synthesis or activation of fully functional G6PD in *Nostoc* sp. strain ATCC 29133. First, the *opcA* mutant strain UCD 366 had only a low level of G6PD activity and its failure to grow under N_2 or in the dark was similar to that of the *zwf* mutant. The phenotype of the *opcA* mutant could be complemented in *trans* by *opcA* alone. An *opcA* mutant phenotype would not have been detected if the other DNA sequence seen hybridizing with *opcA* in Fig. 5B encoded a second OpcA; apparently, either it does not encode a functional OpcA homolog or it was not transcribed under the specific incubation conditions.

Second, in *zwf* mutant strain UCD 341, the presence of *zwf* alone (pSCR122) in *trans* restored only 25% of the wild-type G6PD activity, whereas inclusion of both *zwf* and *opcA* (pSCR123) increased activity approximately 20-fold over that of the wild-type. According to the transcript analysis, a *zwf* mutation should also be polar for *opcA*. Therefore, if OpcA is essential for G6PD activity, one would not predict even partial complementation of a *zwf* mutant strain by pSCR122 (*zwf*). This apparent contradiction can be explained by the presence of a 1.8-kb transcript in strain UCD 341 which hybridized to *opcA* in an RNA blot (data not shown). This band was not seen in RNA preparations from any other strain, and it was most likely due to a fortuitous promoter caused by the *zwf* gene inactivation. The 1.5-kb *opcA* transcript faintly seen in Fig. 2A, lane 4, by the sensitive S1 protection technique was never observed by standard RNA blot hybridization, implying that this promoter plays a minor role in the expression of *opcA* from the chromosome.

RNA blot analysis of the complemented *Nostoc* strains gave no indication of different amounts of *zwf* transcription from pSCR122 (*zwf*) and pSCR123 (*zwf opcA*) (data not shown), implying that OpcA does not act as a transcriptional regulator of this region. This conclusion is also supported by the lack of an identifiable DNA-binding motif. The fact that G6PD activity was restored in the *opcA* mutant by *opcA* alone rules out the possibility that the partial-only complementation of the *zwf*

mutant by *zwf* alone was due to a loss of message stability caused by the 3′ truncation of the normal dicistronic transcript. The enhancement of G6PD activity when *zwf* is expressed together with *opcA* on a multicopy plasmid implies that OpcA might interact directly with G6PD, but we have no evidence to support such a conclusion. Clearly, the role of OpcA in supporting G6PD activity merits further study.

ACKNOWLEDGMENTS

This work was supported by the California Agricultural Experiment Station (project CAD*3620-H) and by the U.S. National Science Foundation (Grant IBN 92-06139).

We are grateful to Norman Hommes for initial isolation of the *Nostoc* sp. strain Mac pDC1 fragment containing the origin of replication and to Peter Wolk, Jeff Elhai, and Yuping Cai for plasmids pRL448 and pRL271; we also thank Kari Hagen, Tom Hanson, and Mike Cohen for critical review of the manuscript. Antibody to the Fe protein of nitrogenase was obtained as a generous gift from J. P. Zehr, Rensselaer Polytechnic Institute.

REFERENCES

1. **Apte, S. K., P. Rowell, and W. D. P. Stewart.** 1978. Electron donation to ferredoxin in heterocysts of the N_2-fixing alga *Anabaena cylindrica*. Proc. R. Soc. Lond. B Biol. Sci. **200:**1–25.
2. **Ausubel, F. M., R. Brent, R. E. Kingston, D. D. Moore, J. G. Seidman, J. A. Smith, and K. Struhl.** 1993. Current protocols in molecular biology. John Wiley & Sons, New York.
3. **Bauer, C. C.** 1994. Ph.D. dissertation. University of Chicago, Chicago, Ill.
4. **Bothe, H., H. Nelles, K.-P. Hager, H. Papen, and G. Neuer.** 1984. Physiology and biochemistry of N_2-fixation by cyanobacteria, p. 199–210. *In* C. Veeger and W. E. Newton (ed.), Advances in nitrogen fixation research. Martinus Nijhoff Publishers, The Hague.
5. **Bothe, H., and G. Neuer.** 1988. Electron donation to nitrogenase in heterocysts. Methods Enzymol. **167:**496–501.
6. **Boyer, H. W., and D. Roulland-Dussoix.** 1969. A complementation analysis of the restriction and modification of DNA in *E. coli*. J. Mol. Biol. **41:**459–472.
7. **Bradford, M. M.** 1976. A rapid and sensitive method for the quantitation of microgram quantities of protein utilizing the principle of protein-dye binding. Anal. Biochem. **72:**248–254.
8. **Brendel, V., and E. N. Trifonov.** 1984. A computer algorithm for testing potential prokaryotic terminators. Nucleic Acids Res. **12:**4411–4427.
9. **Broedel, S. E., Jr., and R. E. Wolf, Jr.** 1990. Genetic tagging, cloning, and DNA sequence of the *Synechococcus* sp. strain PCC 7942 gene (*gnd*) encoding 6-phosphogluconate dehydrogenase. J. Bacteriol. **172:**4023–4031.
10. **Broedel, S. E., Jr., and R. E. Wolf, Jr.** 1991. Growth-phase-dependent induction of 6-phosphogluconate dehydrogenase and glucose 6-phosphate dehydrogenase in the cyanobacterium *Synechococcus* sp. PCC7942. Gene **109:**71–79.
11. **Brusslan, J., and R. Haselkorn.** 1988. Molecular genetics of herbicide resistance in cyanobacteria. Photosynth. Res. **17:**115–124.
12. **Buikema, W. J., and R. Haselkorn.** 1991. Isolation and complementation of nitrogen fixation mutants of the cyanobacterium *Anabaena* sp. strain PCC 7120. J. Bacteriol. **173:**1879–1885.
13. **Cai, Y. P., and C. P. Wolk.** 1990. Use of a conditionally lethal gene in *Anabaena* sp. strain PCC 7120 to select for double recombinants and to entrap insertion sequences. J. Bacteriol. **172:**3138–3145.
14. **Cangelosi, G. A., C. M. Joseph, J. J. Rosen, and J. C. Meeks.** 1989. Cloning and expression of a *Nostoc* sp. leucine biosynthetic gene in *Escherichia coli*. Arch. Microbiol. **145:**315–321.
15. **Cohen, M. F., J. G. Wallis, E. L. Campbell, and J. C. Meeks.** 1994. Transposon mutagenesis of *Nostoc* sp. strain ATCC 29133, a filamentous cyanobacterium with multiple cellular differentiation alternatives. Microbiology (Reading) **140:**3233–3240.
16. **Cossar, J. D., A. J. Darling, S. M. Ip, P. Rowell, and W. D. P. Stewart.** 1985. Immunocytochemical localization of thioredoxins in the cyanobacteria *Anabaena cylindrica* and *Anabaena variabilis*. J. Gen. Microbiol. **131:**3029–3035.
17. **Cossar, J. D., P. Rowell, and W. D. P. Stewart.** 1984. Thioredoxin as a modulator of glucose-6-phosphate dehydrogenase in a N_2-fixing cyanobacterium. J. Gen. Microbiol. **130:**991–998.
18. **Doolittle, W. F.** 1979. The cyanobacterial genome, its expression, and the control of that expression, p. 1–102. *In* A. H. Rose and J. G. Morris (ed.), Microbial physiology, vol. 20. Academic Press, London.
19. **Doolittle, W. F., and R. A. Singer.** 1974. Mutational analysis of dark endogenous metabolism in the blue-green bacterium *Anacystis nidulans*. J. Bacteriol. **119:**677–683.
20. **Elhai, J., and C. P. Wolk.** 1988. A versatile class of positive-selection vectors based on the nonviability of palindrome-containing plasmids that allows cloning into long polylinkers. Gene **68:**119–138.
21. **Ernst, A., T. Black, Y. Cai, J.-M. Panoff, D. N. Tiwari, and C. P. Wolk.** 1992. Synthesis of nitrogenase in mutants of the cyanobacterium *Anabaena* sp. strain PCC 7120 affected in heterocyst development or metabolism. J. Bacteriol. **174:**6025–6032.
22. **Ernst, A., S. Reich, and P. Boger.** 1990. Modification of dinitrogenase reductase in the cyanobacterium *Anabaena variabilis* due to C starvation and ammonia. J. Bacteriol. **172:**748–755.
23. **Favaloro, J., R. Treisman, and R. Kamen.** 1980. Transcription maps of polyoma virus-specific RNA: analysis by two-dimensional nuclease S1 gel mapping. Methods Enzymol. **65:**718–749.
24. **Fay, P.** 1992. Oxygen relations of nitrogen fixation in cyanobacteria. Microbiol. Rev. **56:**340–373.
25. **Grant, S. G., F. R. Jesse, F. R. Bloom, and D. Hanahan.** 1990. Differential plasmid rescue from transgenic mouse DNAs into *Escherichia coli* methylation-restriction mutants. Proc. Natl. Acad. Sci. USA **87:**4645–4649.
26. **Jobling, M. G., and R. K. Holmes.** 1990. Construction of vectors with the p15a replicon, kanamycin resistance, inducible *lacZ*a and pUC18 or pUC19 multiple cloning sites. Nucleic Acids Res. **18:**5315–5316.
27. **Lambert, G., and N. Carr.** 1983. A restriction map of pDC1 from the filamentous cyanobacterium *Nostoc* sp. Mac PCC 8009. Plasmid **10:**196–198.
28. **Lex, M., and N. G. Carr.** 1974. The metabolism of glucose by heterocysts and vegetative cells of *Anabaena cylindrica*. Arch. Microbiol. **101:**161–167.
29. **Margheri, M. C., and G. Allotta.** 1993. Homoacetic fermentation in the cyanobacterium *Nostoc* sp. strain Cc from *Cycas circinalis*. FEMS Microbiol. Lett. **111:**213–218.
30. **Meeks, J. C., K. L. Wycoff, J. S. Chapman, and C. S. Enderlain.** 1983. Regulation of expression of nitrate and dinitrogen assimilation by *Anabaena* species. Appl. Environ. Microbiol. **45:**1351–1359.
31. **Moezelaar, R., and L. J. Stal.** 1994. Fermentation in the unicellular cyanobacterium *Microcystis* PCC 7806. Arch. Microbiol. **162:**63–69.
32. **Neuer, G., and H. Bothe.** 1982. The pyruvate:ferredoxin oxidoreductase in heterocysts of the cyanobacterium *Anabaena cylindrica*. Biochim. Biophys. Acta **716:**358–365.
33. **Neuer, G., and H. Bothe.** 1983. Anaplerotic reactions in *Anabaena cylindrica*. FEBS Lett. **158:**79–83.
34. **Papen, H., G. Neuer, M. Refaian, and H. Bothe.** 1983. The isocitrate dehydrogenase from cyanobacteria. Arch. Microbiol. **134:**73–79.
35. **Parke, D.** 1990. Construction of mobilizable vectors derived from plasmids RP4, pUC18 and pUC19. Gene **93:**135–137.
36. **Pelroy, R. A., and J. A. Bassham.** 1972. Photosynthetic and dark carbon metabolism in unicellular blue-green algae. Arch. Microbiol. **86:**25–38.
37. **Pelroy, R. A., and J. A. Bassham.** 1973. Kinetics of glucose incorporation by *Aphanocapsa* 6714. J. Bacteriol. **115:**943–948.
38. **Pelroy, R. A., G. A. Levine, and J. A. Bassham.** 1976. Kinetics of light-dark CO_2 fixation and glucose assimilation by *Aphanocapsa* 6714. J. Bacteriol. **128:**633–643.
39. **Peschek, G. A.** 1987. Respiratory electron transport, p. 119–161. *In* P. Fay and C. Van Baalen (ed.), The cyanobacteria. Elsevier, Amsterdam.
40. **Rippka, R., J. Deruelles, J. B. Waterbury, M. Herdman, and R. Y. Stanier.** 1979. Generic assignments, strain histories and properties of pure cultures of cyanobacteria. J. Gen. Microbiol. **111:**1–61.
41. **Rippka, R., and M. Herdman.** 1992. Pasteur Culture Collection of Cyanobacteria in Axenic Culture, p. 44–57. Institut Pasteur, Paris.
42. **Sanchez, J. J., N. J. Palleroni, and M. Doudoroff.** 1975. Lactate dehydrogenase in cyanobacteria. Arch. Microbiol. **104:**57–65.
43. **Scanlan, D. J., J. Newman, M. Sebaihia, N. H. Mann, and N. G. Carr.** 1992. Cloning and sequence analysis of the glucose-6-phosphate dehydrogenase gene from the cyanobacterium *Synechococcus* PCC 7942. Plant Mol. Biol. **19:**877–880.
44. **Scanlan, D. J., S. Sundaram, J. Newman, N. H. Mann, and N. G. Carr.** 1995. Characterization of a *zwf* mutant of *Synechococcus* sp. strain PCC 7942. J. Bacteriol. **177:**2550–2553.
45. **Schaeffer, F., and R. Y. Stanier.** 1978. Glucose-6-phosphate dehydrogenase of *Anabaena* sp. Arch. Microbiol. **116:**9–19.
46. **Schmidt-Goff, C. M., and N. A. Federspeil.** 1993. In vivo and in vitro footprinting of a light-regulated promoter in the cyanobacterium *Fremyella diplosiphon*. J. Bacteriol. **175:**1806–1813.
47. **Smith, A. J.** 1982. Modes of cyanobacterial carbon metabolism, p. 47–86. *In* N. G. Carr and B. A. Whitton (ed.), The biology of cyanobacteria. Blackwell Scientific Publications, Oxford.
48. **Summers, M. L., J. C. Meeks, S. Chu, and R. E. Wolf, Jr.** 1995. Nucleotide sequence of an operon in *Nostoc* sp. strain ATCC 29133 encoding four genes of the oxidative pentose phosphate cycle. Plant Physiol. (Bethesda) **107:**267–268.
49. **Sutherland, J. M., M. Herdman, and W. D. P. Stewart.** 1979. Akinetes of the cyanobacterium *Nostoc* PCC 7524: macromolecular composition, structure and control of differentiation. J. Gen. Microbiol. **115:**273–287.
50. **Tacon, W., S. Bharma, B. Sunar, and D. Sherratt.** 1981. Structure and function of plasmid ColK. Plasmid **6:**358–359.
51. **Udvardy, J., G. Borbely, A. Juhasz, and G. L. Farkas.** 1984. Thioredoxins and

the redox modulation of glucose-6-phosphate dehydrogenase in *Anabaena* sp. strain PCC 7120 vegetative cells and heterocysts. J. Bacteriol. **157:**681–683.

52. **Van der Oost, J., B. A. Bulthusis, S. Feitz, K. Krab, and R. Kraayenhof.** 1989. Fermentation metabolism of the unicellular cyanobacterium *Cyanothece* PCC 7822. Arch. Microbiol. **152:**415–419.
53. **Winkenbach, F., and C. P. Wolk.** 1973. Activities of enzymes of the oxidative and the reductive pentose phosphate pathways in heterocysts of a blue-green alga. Plant Physiol. (Bethesda) **52:**480–483.
54. **Wolk, C. P.** 1968. Movement of carbon from vegetative cells to heterocysts in *Anabaena cylindrica*. J. Bacteriol. **96:**2138–2143.
55. **Yates, M. G.** 1992. The enzymology of molybdenum-dependent nitrogen fixation, p. 685–735. *In* G. Stacy, R. H. Burris, and H. J. Evans (ed.), Biological nitrogen fixation. Chapman & Hall, New York.
56. **Zehr, J. P., M. Wyman, V. Miller, L. Duguay, and D. G. Capone.** 1993. Modification of the Fe protein of nitrogenase in natural populations of *Trichodesmium thiebautii*. Appl. Environ. Microbiol. **59:**669–676.